Journal of Visualized Experiments

Neutron Radiography and Computed Tomography of Biological Systems at The Oak Ridge National Laboratory's High Flux Isotope Reactor

--Manuscript Draft--

Article Type:	Invited Methods Collection - JoVE Produced Video
Manuscript Number:	JoVE61688R2
Full Title:	Neutron Radiography and Computed Tomography of Biological Systems at The Oak Ridge National Laboratory's High Flux Isotope Reactor
Corresponding Author:	Hassina Z Bilheux, Ph.D. Oak Ridge National Laboratory Oak Ridge, Tennessee UNITED STATES
Corresponding Author's Institution:	Oak Ridge National Laboratory
Corresponding Author E-Mail:	bilheuxhn@ornl.gov
Order of Authors:	Hassina Z Bilheux, Ph.D.
	Maria Cekanova
	Jeffrey M. Warren
	Matthew J. Meagher
	Ryan Ross
	Jean C. Bilheux
	Singanallur Venkatakrishnan
	Jiao Y.Y. Lin
	Yuxuan Zhang
	Matthew R. Pearson
	Erik Stringfellow
Additional Information:	
Question	**Response**
Please indicate whether this article will be Standard Access or Open Access.	Open Access (US$4,200)
Please indicate the **city, state/province, and country** where this article will be **filmed**. Please do not use abbreviations.	Oak Ridge, TN, USA
Please confirm that you have read and agree to the terms and conditions of the author license agreement that applies below:	I agree to the Author License Agreement
Please specify the section of the submitted manuscript.	Biology
Please provide any comments to the journal here.	

TITLE:

Neutron Radiography and Computed Tomography of Biological Systems at The Oak Ridge National Laboratory's High Flux Isotope Reactor

AUTHORS AND AFFILIATIONS:

Hassina Z. Bilheux[1*], Maria Cekanova[2,3,4*], Jeffrey M. Warren[5*], Matthew J. Meagher[6], Ryan Ross[6], Jean C. Bilheux[1,7], Singanallur Venkatakrishnan[8], Jiao Y. Y. Lin[1,9], Yuxuan Zhang[1], Matthew R. Pearson[9,10], Erik Stringfellow[1]

[1]Neutron Scattering Division, Oak Ridge National Laboratory, Oak Ridge, TN, USA
[2]College of Veterinary Medicine, The University of Tennessee, Knoxville, TN, USA
[3]UT-ORNL Graduate School of Genome, Science and Technology, The University of Tennessee, Knoxville, TN, USA
[4]Now at Integrity Laboratories, Knoxville, TN, USA
[5]Environmental Sciences Division, Oak Ridge National Laboratory, Oak Ridge, TN, USA
[6]Department of Cell & Molecular Medicine, Rush Medical College, Rush University, Chicago, IL, USA
[7]Computer Science and Mathematics Division, Oak Ridge National Laboratory, Oak Ridge, TN, USA
[8]Electrical and Electronics Systems Research Division, Oak Ridge National Laboratory, Oak Ridge, TN, USA
[9]Now at Second Target Station Project, Oak Ridge National Laboratory, Oak Ridge, TN, USA
[10]Neutron Technologies Division, Oak Ridge National Laboratory, Oak Ridge, TN, USA

*These authors contributed equally.

E-mail addresses of co-authors:

Maria Cekanova	(mcekanov@utk.edu)
Jeffrey M. Warren	(warrenjm@ornl.gov)
Matthew J. Meagher	(matthew.j.meagher@gmail.com)
Ryan Ross	(Ryan_Ross@rush.edu)
Jean C. Bilheux	(bilheuxjm@ornl.gov)
Singanallur Venkatakrishnan	(venkatakrisv@ornl.gov)
Jiao Y. Y. Lin	(linjiao@ornl.gov)
Yuxuan Zhang	(zhangy6@ornl.gov)
Matthew R. Pearson	(pearsonmr@ornl.gov)
Erik Stringfellow	(stringfellde@ornl.gov)
Hassina Z. Bilheux	(bilheuxhn@ornl.gov)

Corresponding Author:

Hassina Z. Bilheux (bilheuxhn@ornl.gov)

KEYWORDS:

neutron radiography, neutron computed tomography, reactor source, neutron imaging, image data reconstruction, visualization, detectors, biological samples

SUMMARY:
This manuscript describes a protocol for neutron radiography and computed tomography of biological samples using a High Flux Isotope Reactor (HFIR) CG-1D beamline to measure a metal implant in a rat femur, a mouse lung, and an herbaceous plant root/soil system.

ABSTRACT:
Neutrons have historically been used for a broad range of biological applications employing techniques such as small-angle neutron scattering, neutron spin echo, diffraction, and inelastic scattering. Unlike neutron scattering techniques that obtain information in reciprocal space, attenuation-based neutron imaging measures a signal in real space that is resolved on the order of tens of micrometers. The principle of neutron imaging follows the Beer-Lambert law and is based on the measurement of the bulk neutron attenuation through a sample. Greater attenuation is exhibited by some light elements (most notably, hydrogen), which are major components of biological samples. Contrast agents such as deuterium, gadolinium, or lithium compounds can be used to enhance contrast in a similar fashion as it is done in medical imaging, including techniques such as optical imaging, magnetic resonance imaging, X-ray, and positron emission tomography. For biological systems, neutron radiography and computed tomography (CT) have increasingly been used to investigate the complexity of the underground plant root network, its interaction with soils, and the dynamics of water flux in situ. Moreover, efforts to understand contrast details in animal samples, such as soft tissues and bones, have been explored. This manuscript focuses on the advances in neutron bioimaging such as sample preparation, instrumentation, data acquisition strategy, and data analysis using a High Flux Isotope Reactor (HFIR) CG-1D beamline. The aforementioned capabilities will be illustrated using a selection of examples in plant physiology and biomedical applications.

INTRODUCTION:
The principle of neutron radiography (nR) is based on the attenuation of neutrons through the matter that they traverse. Unlike X-rays that are scattered by the electron cloud of an atom, neutrons can be absorbed or scattered by its nucleus. Neutrons are sensitive to light elements, such as hydrogen (H), and can consequently be used to radiograph biological applications such as imaging of animal[1–7] or human tissues[8,9] and below-ground soil/root systems[10–15]. Neutron imaging is a complementary technique to X-ray imaging, which is capable of detecting heavy elements[16–18]. Attenuation-based nR is governed by the linear attenuation coefficients of the materials within the sample and by the thickness of the sample, as described by the Beer-Lambert law, which states that the transmitted beam is directly proportional to the amount of material and the path length through the material. Thus, the transmittance, *T*, can be calculated as:

$$T = \frac{I}{I_0} = e^{-\mu x} \quad (1)$$

where I_0 and I are, respectively, the incident and transmitted beam intensities; μ and x are the linear attenuation coefficient and the thickness of a homogeneous sample, respectively. The attenuation coefficient μ is given by:

$$\mu = \sigma \frac{\rho N_A}{M} \quad (2)$$

where σ is the sample's neutron attenuation cross-section (both scattering and absorption), ρ is its density, N_A is Avogadro's number, and M is its molar mass.

Contrast in radiography of biological samples using low-energy neutrons (i.e., energies below 0.5 eV) is mostly due to a change in the density of H (for a fixed sample thickness). This is due to the probability of interaction of a neutron with the H nucleus, which is greater than with other nuclei present in biological samples, and the fact that the density of the H atom is paramount as it is the most abundant atom in biological samples.

Since its early stages, nR and neutron computed tomography (nCT) have been extensively used for materials and engineering applications[19–23]. The first demonstration experiments of neutron sensitivity to H in biological samples began in the mid-1950s[24] with the measurements of plant specimens. The work continued through the 1960s with, for example, the radiography of a human chest[25] or rats[26], in which the use of contrast agents, such as gadolinium oxide (Gd_2O_3), was explored. Moreover, it was hypothesized that contrast in human tumor tissue versus normal tissue was due to a local increase in H content. During these initial trials, it was concluded that increased neutron flux and spatial resolution would improve the quality of nR and would likely increase its popularity as a complementary technique for industrial or biomedical applications. The most recent studies comprise nR and nCT measurements performed on cancer tissue specimens[1] and sections of animal organs[2,3,27] for biomedical and forensic applications.

Located at the Oak Ridge National Laboratory, Oak Ridge, TN, the HFIR is a powerful neutron source that produces neutrons by fission reaction. These neutrons have energies in the order of 2 MeV and are "cooled" in the reactor pool by kinetic reactions with heavy water to reach energies in the order of 100–300 eV. The optimization of a neutron experiment, whether scattering or imaging, starts with the understanding of the neutron source and beamline properties such as its beam intensity and energy distribution and the effect of background (fast neutrons, delayed neutrons, gamma rays). In the HFIR cold guide hall where the imaging beamline is located, neutrons are further "cooled" by kinetic interactions with a liquid H moderator. They are then transported in a curved guide system away from the line of sight of the source, thus eliminating fast neutrons and gamma pollution. As illustrated in **Figure 1**, the CG-1D neutron-imaging beamline[28,29] is placed on a cold guide, implying that the neutron energy range varies from a few meV to a few tens of eV (in this case, the corresponding usable neutron wavelength ranges from 0.8 to 10 Å) with a flux in the range of 10^7 n/(cm^2·s) at the sample position.

Finally, neutrons that have not interacted with the sample are collected in a beam stop position,

approximately 1 m downstream from the detector system to minimize background noise. The CG-1D beam stop is 0.75 m wide, 0.5 m tall, and 35 mm thick and is made of boron carbide in epoxy. The beam stop is reinforced with 10 mm of 95% enriched lithium carbonate ($^{6}Li_2CO_3$) in a fire-resistant epoxy where the neutron beam hits, with a cavity lined with ^{6}Li, Pb, and steel designed to contain the high rate of secondary gamma rays. The beam stop is directly attached to the steel shielding wall of the beamline. A photograph of the CG-1D beamline is given in **Figure 2**.

This manuscript aims to demonstrate the procedure of using neutron imaging (nR and nCT) at the High Flux Isotope Reactor (HFIR) CG-1D beamline. This study also illustrates the current state-of-the-art nR and nCT capabilities for biological samples, specifically a mouse lung, a rat bone, and plant root/soil systems. The mouse lung was chosen to illustrate the complementarity of neutrons to measure the lung tissue, whereas X-rays are mostly sensitive to bones. The bone sample, a rat femur, had a titanium (Ti) implant, thus illustrating the contrast between the bone and the metal, and the opportunity to see the bone/metal interface (which is difficult to measure with X-rays as metals strongly attenuate them[4]). Finally, the plant-root water system illustrates the three-dimensional (3D) capability of nCT to measure root/soil systems in situ. It additionally shows the advantages/disadvantages of using nR for biological samples. Evidently, this method can be safely used to measure water dynamics in a plant-root system, but cannot be considered as a live animal and human imaging technique due to the risks associated with radiation exposure, thus limiting studies to either (dead) mice or pathology-like measurements wherein, for example, a tissue sample is resected from a patient (animal or human) and prepared by fixation before being measured in a neutron beam.

PROTOCOL:

1. **Instrument setup** (see **Figure 3**, section 3)

1.1. On the beamline computer, open a terminal window, type **css**, and then press **Enter** to launch the user interface.

1.2. If not opened by default, choose the **User Home** option in the **Menu** tab to open the **Experimental Physics and Industrial Control System (EPICS) Imaging Interface**.

1.3. Using the first tab (called **Proposal/Camera/SE Device**) of the interface, select the beamline optics by clicking on the **Optics** button next to **Camera/Detectors**, i.e., the **pinhole aperture size** and **opening of the slit system** by clicking on the **Slits** button.

1.4. Bolt the rotation stage onto the XY stages, where the sample is to be placed, and position the detector (sCMOS or CCD).

1.4.1. For the CCD or the sCMOS detector, select the lens with the magnification that provides the desired spatial resolution and focal length, in consultation with the instrument team. Using light first, focus the camera by either moving the detector closer or further from the mirror, or

by manually tuning the lens at a fixed detector position. Focus the image at the location of the neutron scintillator.

1.4.2. For the CCD or the sCMOS detector, fine-tune the lens focus with neutrons using a neutron-absorbing resolution mask[30] placed against the detector scintillator. Collect successive radiographs using different settings (i.e., different detector positions from the mirror automated by moving the **detector** motor in EPICS).

1.4.4. Compare radiographs by evaluating line pairs in ImageJ/Fiji[31] or a similar image software tool.

1.5. When appropriate, secure the sample in a suitable container (Al container and/or Al heavy-duty foil), placing the sample on the rotation stage as close as possible to the detector. Shield the detector and equipment using neutron (boron rubber) and gamma (Pb bricks) shielding.

1.6. Measure the sample-to-detector distance, and remove the sample. Replace it with the resolution mask to evaluate the pixel size at sample position in this beamline configuration. Using a known feature dimension, evaluate the number of pixels across the feature to determine the pixel size.

1.7. Reposition the sample on the rotation stage.

1.8. Using the EPICS interface and the **Align Sample** tab, align the sample with the neutron beam by taking successive fast (ms to 1 s) radiographs while the sample is moving until it is in full view of the detector. Save the sample alignment file, which will be reused before the CT scan starts.

1.9. Before starting the CT scan, use the automated **CT Alignment Check** option (in the **Alignment** tab) to verify that the sample remains in the field-of-view at different angles by assessing radiographs as they are generated at different sample orientations with the beam.

2. Specimen preparation and data acquisition strategy

2.1. Rat femurs

2.1.1. Implant Ti_6Al_4V rods (1.5 mm diameter and 15 mm length) into the femurs of male Sprague-Dawley rats, placing them within the intramedullary space through the distal femoral condyles.

2.1.2. Sacrifice the rats after 12 weeks, and harvest the femurs. Remove all soft tissue (which contributes to neutron attenuation), and freeze the femurs with implants in saline-soaked gauze. Fully submerge 2-inch squared gauze sponges in phosphate-buffered saline (PBS), and wrap each sample fully in these soaked sponges (see the **Table of Materials**).

2.1.3. Thaw the femurs to room temperature for X-ray-based microCT scans[324], before transporting them in a frozen state to the HFIR.

2.1.3.1. Prior to nCT, rethaw the sample, and bring it to room temperature at the HFIR Biohazard Safety Level 2 (BSL2) laboratory located close to the CG-1D neutron imaging beamline. Once at room temperature, wrap the sample in heavy-duty Al foil and place it in an Al cylinder.

2.1.3.2. Position the cylinder vertically on the rotation stage at the beamline, and scan the femur at the beamline at room temperature from 0 to 360°, with a stepping angle of 0.25°. Acquire each radiograph for 50 s.

NOTE: Considering dead time for the rotation stage movement and transfer of each radiograph from the CCD to the data acquisition computer, the total time of the scan was approximately 24 h.

2.1.4. Once the nCT is completed, bring the sample back to the BSL2 lab, remove the containment, and refreeze the sample to preserve it for further experimental measurements.

2.2. Mouse lungs

2.2.1. Resect lung tissue from a dead mouse used for experiments unrelated to this study. Fix the sample in a solution of 70% ethanol prior to the neutron experiments.

2.2.2. Wrap the tissue in heavy-duty Al foil and transport it from the BSL2 lab directly to the CG-1D beamline. Insert the sample in an Al cylinder for double containment and to maintain the sample position in the beam during the nCT scan.

2.2.3. Position the sample close to the CCD, and perform the scan overnight at room temperature.

NOTE: Each radiograph was 150 s, and the rotation stepping angle was 0.5°, from 0 to 182°. The total time for the scan was around 16 h.

2.3. Herbaceous plant root/soil system

NOTE: As with other biological samples, plant-soil systems are limited in size due to the strong attenuation of hydrogen, particularly water in the soil or plant roots. Seeds or ramets may be planted in containers (Al or quartz—both having low neutron attenuation cross-sections), or a more mature plant can be transplanted into a container.

2.3.1. Carefully excavate and transplant a local herb growing onsite (here, mulberry weed (*Fatoua villosa* (Thunb.) Nakai) into an Al container of cross-section of 2.38 cm x 2.58 cm, a height of 6.3 cm, wall thickness of 0.055 cm, and containing pure sand (SiO_2).

2.3.2. Rinse the plant roots with deionized water, and carefully display them within the Al container while filling the container with a slurry of wet sand.

NOTE: When filling containers with soil, it is important to use wet soil, as dry soil will separate out by particle size and create textural artifacts in the containers[12,13].

2.3.3. After planting, measure the saturated weight of the plant system, and weigh the plant system every day to assess the rate of water use. Apply water either to the top surface of the soil or through a port or hole at the bottom of the container using a tube or syringe.

NOTE: Here, the plant system was placed on a scale, and water was applied to the top each day to replace daily water use based on weight. Water can be withheld prior to imaging to reduce soil water content and enhance contrast in the roots.

2.3.4. Propagate the plant system in an onsite growth chamber with controlled temperature and light[12]. Maintain the plant system for 1 week prior to imaging to allow for plant root acclimation to the Al container.

NOTE: Once imaging begins, do not water the plant.

2.3.5. Perform the nCT scans in ~1.75 h each, and continuously scan over a period of 2.5 days to map dynamic 3D changes in soil and plant water content. For these measurements, decrease the spatial resolution to a few hundred μm in favor of time resolution (i.e., faster acquisition time for each projection).

NOTE: Each CT scan was performed with a rotation angle of 0.93° and an acquisition time of 10 s per projection. For the purpose of this manuscript, only the first CT scan is presented.

3. Data acquisition

NOTE: The data acquisition system at CG-1D utilizes the Experimental Physics and Industrial Control System (EPICS) software environment[33]. These protocols were approved by the University of Tennessee's Institutional Animal Care and Use Committee for the mouse lung and the Rush University Medical Center Institutional Animal Care and Use Committee for the rat femur. The EPICS data acquisition protocol is as follows (**Figure 3**). Once the detector and beamline optics are set on the right side of the interface, sample environment (SE) and rotation stages (for CTs) can be selected.

3.1. Select the first **EPICS** tab titled **Proposal/Camera/SE Device**. Click on the **Switch Proposal or Sample** button. Select the **project number** and **sample ID#** to be measured in the **List of Proposals** (left) and **Sample** (right) that have replaced the previous tab.

3.2. Use the **back arrow** to come back to the main EPICS interface. Select the **detector** to be

used (sCMOS or CCD) by choosing one of the four available detectors (Andor CCD, Andor sCMOS, SBIG CCD, or MCP) in the **Camera/Detector** option list.

NOTE: The SBIG CCD is used for testing by the instrument and can be ignored for the present manuscript.

3.3. Select the rotation stage to be used in the **Sample Environment Device** section.

3.3.1. First, click on **Rotation Stage (CT Scan)** in the **Sample Environment Device** list. Then, select one of the rotation stages (which corresponds to the sample to be scanned).

3.4. Finally, at the bottom of the tab, select the **Data Acquisition Mode**. In this case, select the first option, **White Beam**.

NOTE: The mode of acquisition is either white beam (taking the whole range of neutron wavelength) or monochromatic at the CG-1D beamline.

3.5. Select the second EPICS tab titled **Align Sample**. Type a sample file name, and press **Enter**. Repeat the process for the sub folder name.

NOTE: The EPICS interface is programmed to automatically save data in the proper experimental directories, which the in-house reconstruction software uses to produce 2-dimensional (2D) slices of the 3D object under investigation. The second tab, **Align Sample**, allows the alignment of the sample using radiographs that are a few seconds only as these radiographs are not used later for data processing and analysis. Once all motors are positioned properly, their positions can be saved in a .csv file format; thus, each sample alignment has its corresponding .csv file that can be called back to position the samples for CT scans at a later time.

3.6. Skip the alignment of the three motors, i.e., assume that the sample is aligned and ready for CT. Select a desired acquisition time, and click on the **Take Quick Images** button. Collect a series of radiographs with different acquisition times to evaluate signal-to-noise ratio (SNR).

3.7. Open ImageJ/Fiji; drag and drop the different radiographs. Plot a profile going from the sample to an open area; evaluate SNR.

3.8. If multiple samples are set on the XY stage (multiple rotation stages, each for one sample), record each sample position after alignment, and save the data as .cvs file by clicking on the **Save in a File** button.

3.9. Select the third EPICS tab titled **Collect Data** to set up the CT scan parameters. Type a file name on the first writable line, and press **Enter**. Repeat for the sub-folder name.

NOTE: The layout of the **Collect Data** tab depends on the selection of a series of time-elapsed radiographs (no SE) or CT scans (selection of a rotation stage) in the first tab.

3.10. In the **Align Sample Using the Saved File** section, select the file that previously recorded the sample motor positions (step 1.8). Use the **Recently Saved Files** to browse through the recently saved sample alignment files. Click on **Align Using File** to make the sample go back in position in the neutron beam.

3.11. Calculate the number of projections required for the CT based on Nyquist's sampling theorem. Calculate the number of pixels across the sample horizontal dimension, and multiply by 1.5 to obtain the number of needed projections to fulfill Nyquist's sampling.

3.12. Enter the **Rotation Start Angle** (usually 0°), **Rotation End Angle** (usually 180°), **Rotation Step Size**, the **Number of Images per Step** (usually set to 1), and the **Exposure time** for each image. Start the CT scan by clicking on the **Collect Data** button.

4. Volume reconstruction and data processing/analysis

NOTE: All CG-1D software tools for data normalization, reconstruction, and analysis are available on the ORNL facility's Python repository and on the facility's analysis servers. For 2D measurements, pre-processing can be done using Jupyter Python notebooks[34]. An illustration of a notebook is available in **Figure 4**.

4.1. Log on to the Linux analysis server using the username and password. Open the web browser, and type **jupyter.sns.gov**.

4.2. Open the python Jupyter notebook named **iMARS3D**. Run the first few lines of the code (which loads the tools necessary to run iMARS3D). Load data, flat, and dark field. Verify that all the three data sets are properly loaded.

4.3. Proceed with cropping the data, filtering (as necessary), normalization (with automated sample tilt correction), and volumetric reconstruction (a long process). Save the data in the project number folder named **Shared**. After turning on AMIRA[35], which is also available on the facility analysis servers, load the reconstructed slices in the software, and proceed with visualization, further filtering, and analysis.

REPRESENTATIVE RESULTS:

A custom-designed interface was developed to guide the experimental protocol and minimize human error; this interface logically steps through the different necessary steps prior to measuring a sample. As illustrated in **Figure 3**, the interface is divided in three major sections: left, center, and right. The left section provides a status of the ongoing experiment, along with motor positions and experimental details (sample information, proposal number, and team members). Each experiment is associated with a proposal number and one or multiple samples. Proposal information, such as team members and selected sample name, are also available on the right side (first tab named **Proposal/Camera/Sample Environment Device**). The center

section comprises the current radiograph with a dynamic range scale bar on the side, along with status and log information below the image.

Figure 5A is a photograph of a representative rat femur of similar size as the one measured; **Figure 5B,C** represent the nCT of a rat's femur with the Ti implant. **Figure 5A** shows the false color attenuation-based nCT of the femur, while **Figure 5B** represents a diagonal cut through the bone with the same orientation as in **Figure 5A** to reveal the Ti implant (in gray scale) resembling an X-ray medical CT. This implant does not interact with neutrons as much as the bone material; thus, its attenuation is minimum, and it appears darker (i.e., less attenuating) than the surrounding bone. Trabecular bone, which is present within the medullary space of the femur, is clearly visible at the proximal end of the sample (red arrows in **Figure 5B**).

Figure 6A,B show representative photographs of the ethanol-fixed mouse lung, in two different positions, used for nCT to demonstrate the ability of neutrons to detect soft tissue specimens. The reconstructed volume of the mouse lung obtained from nCT are shown in **Figure 6C,D**, positioned in a similar fashion as **Figure 6A,B**. A cut through the right lobe of the lung is illustrated in **Figure 6E**. Despite the relatively small size of the sample, neutron sensitivity is clearly demonstrated by a detection of structure of lung at ~75 µm spatial resolution. As expected, the range of attenuation is quite broad, with a large portion corresponding to a low to medium neutron attenuation as lungs have a sponge-like structure containing air.

Figure 7A shows a photograph of the plant sample, while **Figure 7B** represents the false color volumetric rendering of the plant root/soil system in a rectangular Al container (which is not visible because Al is mostly transparent to neutrons). Compared to the previous data sets, SNR is poorer, as expected, as the data were acquired faster to track the dynamic movements of water uptake in the root in 3D over 2.5 days. Thus, each CT scan was optimized to be measured within a ~1.75 h window. Despite poor SNR, the root system in soil is clearly visible in the vertical cuts of the sample displayed in **Figure 7C,D** in false color.

FIGURE AND TABLE LEGENDS:

Figure 1: Schematic drawing of the HFIR CG-1D neutron imaging beamline. The imaging beam is defined by the aperture system that defines a cone beam geometry. The beam is transported via a He-filled flight tube with beam scrapers to remove unwanted stray neutrons. A borated rubber liner inside the flight tube decreases background from neighboring beamlines. Abbreviations: HFIR = High Flux Isotope Reactor; He = helium; L = distance from the pinhole aperture of diameter, D, and the detector.

Figure 2: The CG-1D neutron imaging facility at the High Flux Isotope Reactor. The photograph shows, front right to left, the flight tubes, sample area, and beam stop. The neutron beam is coming from the right side of the photograph. The flight tube has been signed by the scientific and industry research community that utilize the instrument.

Figure 3: EPICS interface. The CG-1D EPICS interface is divided into three sections: the status

section (left), the display area (in this example, a raw radiograph of a brass nautical sundial), and the parameter input for 2D and 3D imaging. Abbreviations: EPICS = Experimental Physics and Industrial Control System; 2D = two-dimensional; 3D = three-dimensional.

Figure 4: A screenshot of a Jupyter notebook. This notebook is utilized to preview a set of radiographs before normalizing them. In this example, the same brass nautical sundial shown in **Figure 3** is visualized.

Figure 3: **Rat femur with titanium implant.** (**A**) Photograph of a representative rat femur. (**B**) 3D rendered volume of rat femur obtained from nCT. (**C**) Diagonal slice showing the titanium rod inside the femur. Red arrows show the trabecular bone. The scale bars are presented by the x and y axes, respectively.

Figure 4: Mouse lung nCT. (**A**) and (**B**) Representative photographs of mouse lung. (**C**) and (**D**) Attenuation-based 3D rendered volume of mouse using the same positioning as (**A**) and (**B**). (**E**) Representative slice through the right lobe of the mouse lung (**D**) showing a structure of lung obtained with a different gradient of neutron attenuation (mostly low attenuation).

Figure 5: Neutron computed tomography and slices through the plant root/soil system. (**A**) Photograph of plant sample. (**B**) 3D rendered volume from neutron computed tomography of the plant showing the stem above ground, and the soil system with water (in red). (**C**) and (**D**) are cuts through the sample angled to show the stem and roots in the soil (red arrows). Darker blue areas in the soil indicate the presence of water.

DISCUSSION:

Neutron radiography and CT of biological samples are promising imaging techniques that are complementary to X-ray imaging or magnetic resonance imaging. The critical steps in performing a neutron imaging experiment of a biological sample are related to its preparation and its containment at the beamline. Optimization of an experiment is driven by the scientific question to be answered. If the science question requires high spatial resolution to observe a phenomenon, then long acquisition times are required, and the drawback of nCT (with cm size field-of-view) is that it takes hours to perform a scan. This is mostly due to the difference in overall neutron flux available at a reactor compared to a synchrotron source, where X-ray CT scans can take seconds to minutes for a few mm^2 field-of-view. Although the method can be applied to ex vivo tissue samples extracted from animals, it cannot be extended in vivo to live animals or humans due to the radiation exposure risk (such as gamma rays produced by neutrons and neutron interactions with the atoms in the sample). However, it is well-suited for the imaging of plant root/soil interactions (**Figure 7**) such as water uptake dynamics.

The advantage of using fast nCT for plant dynamics is the sensitivity to H in water and the absence of radiation damage to the plant, unlike X-ray CT. Moreover, unique contrast can be observed from the use of neutrons in bone/metal samples such as a rat femur where the metal is relatively transparent compared to the surrounding tissues (**Figure 5**), potentially avoiding metal artifacts induced by X-ray CT[32]. Animal tissues, such as mouse lung, show impressive detection of soft

tissue structure because neutrons are sensitive to H, but spatial resolution is somewhat the limiting factor in these measurements. Contrast is provided by the H atoms present in biological samples[19,32]. A motorized aperture/diffuser system defines the pinhole geometry of the imaging instrument. Neutrons travel a distance of 6.59 m in a helium (He)-filled flight tube with aluminum (Al) windows on each end. Flight tubes are used to transport neutrons, while limiting air scatter, such that the loss in beam intensity is minimum. For the measurements described in this manuscript, the diffuser is made of a 1 mm-thick 50 nm Al_2O_3 nano-powder encased in an Al container. The diffuser reduces beam artifacts coming from the neutron guide (which are magnified by the pinhole geometry of an imaging beamline). Otherwise, sharp horizontal and vertical intensity fluctuations are visible in the radiograph, and normalization of the data becomes challenging. For the experiments illustrated here, neutrons are converted to light using a 25-μm-thick lithium-6 fluoride/zinc sulfide phosphor (^{6}LiF/ZnS:Ag).

Collimation optimization depends on the sample-to-detector position, the required spatial resolution, and acquisition time. When the sample sits a few cm away from the scintillator, high collimations (L/D above 800, where L is the distance from the pinhole aperture of diameter, D, and the detector) yield better spatial resolution at the cost of neutron flux. Low collimation (L/D below 800) is preferable for in situ dynamic studies when time resolution prevails over spatial resolution. For the measurements described in this manuscript, L/D and spatial resolution were approximately 355 and 75 μm, respectively. Temporal resolution varied based on the SNR. The sample was positioned as close to the scintillator as possible to reduce geometrical distortion such as blurring. Translation and rotation stages are available to set the sample close to the detectors and perform CT. CG-1D offers three types of detectors: a charge-coupled device (CCD) with 2048 pixels x 2048 pixels with a pixel pitch of 13.5 μm, a scientific complementary metal-oxide semiconductor (sCMOS) detector with 2560 pixels x 2160 pixels with a pixel pitch of 6.5 μm, and a micro-channel plate (MCP) detector[36,37] with 512 pixels x 512 pixels with a pixel size of 55 μm. Each detector is optimized for a different field-of-view (FOV) as well as spatial and time resolutions. For the rat femur and the mouse lung measurements, the CCD detector was utilized for its large FOV capability (~ 7 cm x 7 cm) and reasonable spatial resolution of approximately 75 μm. The plant root/soil system's nCT was performed with the sCMOS, as the goal was to acquire nCTs as quickly as possible at the cost of FOV (which was limited to ~ 5 cm x 4.2 cm); thus, spatial resolution evidently suffered.

In these detectors, neutrons are either converted to light or an alpha particle for detection purposes. Rotating the sample around its vertical axis and acquiring radiographs at consecutive rotation angles allows the acquisition of nCT. Both the sample and sample holder can produce gamma rays and can scatter neutrons toward the detector. First, neutrons are absorbed with ~5 mm thick boron rubber to protect the detector chip from seeing neutrons. This absorption generates gamma rays that can be stopped by lead (Pb) placed between the boron rubber and the detector. Three reconstruction software applications were used to reconstruct the experimental data in 3D. The mouse lung sample reconstruction was performed using Octopus[38], a commercial reconstruction software that utilizes FBP; however, the license sales and support for Octopus have been discontinued. Octopus software sat on a server PC and could be used to

reconstruct data collected at the beamline. An in-house reconstruction software, named iMARS3D, is now available at CG-1D and replaces Octopus. It is based on the open source code, TomoPY[39], with added features such as automated tilt correction and post-processing filters. iMARS3D includes pre-processing of the data (subtraction of the background and noise), cropping, median filtering (to correct for gamma strikes and dead pixels), and automated beam intensity fluctuation correction.

Once sinograms are created, further data processing, such as ring artifact removal and smoothing, can also be performed. The different steps of the reconstruction are saved on the analysis server (and later moved in the proposal shared folder), while the final 2D slices are immediately stored in the proposal shared folder. The rat femur was reconstructed using iMARS3D. The plant root/soil sample was pre-processed by median filtering the data using the TomoPY followed by tilt axis correction using Python's SciPy library. The reconstruction was carried out using a python package developed in-house pyMBIR built using kernels from the ASTRA toolbox[40], which implements a suite of tomographic algorithms from the baseline FBP to advanced model-based iterative reconstruction techniques[41] that can obtain high quality reconstructions from extremely sparse and noisy neutron data sets, such as the plant fast nCT dataset. All rendered volumes based on the aforementioned reconstruction tools are represented in attenuation contrast. All visualization was performed using the commercial visualization, segmentation, and data analysis software package, AMIRA[35].

For volume reconstruction and data processing and analysis, data can be loaded and previewed before selecting a region of interest outside the sample that is used to normalize to 1 (or 100% transmission) any beam fluctuation. These notebooks can be adapted to each measurement, making pre-processing a straightforward effort. Furthermore, 2D analysis can be performed in the same notebook such as tracking kinetic changes (i.e., water uptake in a sample) in a sample through time. With the advances of novel techniques, such as neutron grating interferometry, and the improvement in spatial resolution (a few microns have recently been reported[42,43] with a few mm^2 size field of views), neutron imaging may offer yet new contrast mechanisms for biological tissues with improved spatial resolution. The exploration of higher energy neutrons (to allow the measurements of thick samples) also promises the ability to measure larger sections of an animal tissue such as an intact mouse, thus offering yet new possibilities for ex vivo biomedical research.

ACKNOWLEDGMENTS:
Part of this research utilized resources at the High Flux Isotope Reactor, operated by ORNL, and sponsored by the U.S. Department of Energy, Office of Science, User Facilities, under contract DE-AC05-00OR22725 with UT-Battelle, LLC. Part of this research was supported by ORNL through the Eugene Wigner Distinguished Staff Fellowship program. This research was also sponsored by the DOE Office of Science, Office of Biological and Environmental Research. Rat femoral samples were obtained from experiments performed in collaboration with Dr. Rick Sumner at Rush University Medical Center with funding obtained from the NIH (R01AR066562) and from the Orthopedic Research and Education Foundation-Smith and Nephew award. The team wants to thank the HFIR support teams that enable the use of the neutron scattering beamlines.

DISCLOSURES:

The authors have nothing to disclose.

REFERENCES:

1. Cekanova, M., Donnell, R., Bilheux, H., Bilheux, J.-C. Neutron imaging: Detection of cancer using animal model. *Proceedings of the 2014 Biomedical Sciences and Engineering Conference - 5th Annual ORNL Biomedical Sciences and Engineering Conference: Collaborative Biomedical Innovations - The Multi-Scale Brain: Spanning Molecular, Cellular, Systems, Cognitive, Behaviour*. doi: 10.1109/BSEC.2014.6867752 (2014).
2. Bilheux, H. Z. et al. Neutron imaging a. The Oak Ridge National Laboratory: Application to biological research. *Proceedings of the 2014 Biomedical Sciences and Engineering Conference - 5th Annual ORNL Biomedical Sciences and Engineering Conference: Collaborative Biomedical Innovations - The Multi-Scale Brain: Spanning Molecular, Cellular, Systems, Cognitive, Behaviour*. doi: 10.1109/BSEC.2014.6867751 (2014).
3. Bilheux, H. Z. et al. A novel approach to determine post mortem interval using neutron radiography. *Forensic Science International*. **251**, doi: 10.1016/j.forsciint.2015.02.017 (2015).
4. Isaksson, H. et al. Neutron tomographic imaging of bone-implant interface: Comparison with X-ray tomography. *Bone*. **103**, 295–301 (2017).
5. Le Cann, S. et al. Characterization of the bone-metal implant interface by Digital Volume Correlation of in-situ loading using neutron tomography. *Journal of the Mechanical Behavior of Biomedical Materials*. **75**, 271–278 (2017).
6. Burca, G. et al. Exploring the potential of neutron imaging for life sciences on IMAT. *Journal of Microscopy*. **272** (3), 242–247 (2018).
7. Metzke, R. W. et al. Neutron computed tomography of rat lungs. *Physics in Medicine and Biology*. **56** (1), 1–10 (2011).
8. Altieri, S. et al. Neutron autoradiography imaging of selective boron uptake in human metastatic tumours. *Applied Radiation and Isotopes*. **66** (12), 1850–1855 (2008).
9. Altieri, S., Bortolussi, S., Bruschi, P., Pedroni, P., Zonta, A. Neutron radiography of human liver metastases after BPA infusion. *Proceedings of 11th World congress on Neutron Capture Therapy* (2004).
10. Holz, M., Zarebanadkouki, M., Kaestner, A., Kuzyakov, Y., Carminati, A. Rhizodeposition under drought is controlled by root growth rate and rhizosphere water content. *Plant and Soil*. **423** (1–2), 429–442 (2018).
11. Esser, H. G., Carminati, A., Vontobel, P., Lehmann, E. H., Oswald, S. E. Neutron radiography and tomography of water distribution in the root zone. *Journal of Plant Nutrition and Soil Science*. **173** (5), 757–764 (2010).
12. Warren, J. M. et al. Neutron imaging reveals internal plant water dynamics. *Plant and Soil*. **366** (1–2) (2013).
13. Dhiman, I. et al. Quantifying root water extraction after drought recovery using sub-mm in situ empirical data. *Plant and Soil*. **424**, 73–89 (2018).
14. Kroener, E., Zarebanadkouki, M., Kaestner, A., Carminati, A. Non-equilibrium dynamics of rhizosphere. *Water Resources Research*. **50** (8), 6479–6495 (2014).

15. Moradi, A. B. et al. Three-dimensional visualization and quantification of water content in the rhizosphere. *New Phytologist*. **192** (3), 653–663 (2011).
16. Banhart, J. et al. X-ray and neutron imaging - Complementary techniques for materials science and engineering. *International Journal of Materials Research*. **101** (9), 1069–1079 (2010).
17. LaManna, J. M., Hussey, D. S., Baltic, E. M., Jacobson, D. L. Improving material identification by combining x-ray and neutron tomography. *Proceedings 10391, Developments in X-Ray Tomography XI*. **1039104** doi: 10.1117/12.2274443 (2017).
18. Tengattini, A. et al. NeXT-Grenoble, the Neutron and X-ray tomograph in Grenoble. *Nuclear Instruments and Methods in Physics Research, Section A: Accelerators, Spectrometers, Detectors and Associated Equipment*. **968**, 163939, doi: 10.1016/j.nima.2020.163939 (2020).
19. *Neutron Imaging and Applications*. Bilheux, H. Z., McGreevy, R. L., Anderson, I. S. (Eds), Springer, Boston, MA, USA, doi: 10.1007/978-0-387-78693-3. (2009).
20. Zhang, P., Wittmann, F. H., Zhao, T. J., Lehmann, E. H., Vontobel, P. Neutron radiography, a powerful method to determine time-dependent moisture distributions in concrete. *Nuclear Engineering and Design*. **241** (12), 4758–4766 (2011).
21. Lobo, R. M., Andrade, A. H. P., Castagnet, M. Hydride embrittlement in zircaloy components. *Inac 2011 Int Nucl.Atlantic Conference*. 1–6 (2011).
22. Kardjilov, N. et al. New trends in neutron imaging. *Nuclear Instruments and Methods in Physics Research, Section A: Accelerators, Spectrometers, Detectors and Associated Equipment*. **605** (1–2), 13–15 (2009).
23. Schillinger, B. et al. Detection systems for short-time stroboscopic neutron imaging and measurements on a rotating engine. *Nuclear Instruments and Methods in Physics Research, Section A: Accelerators, Spectrometers, Detectors and Associated Equipment*. **542** (1–3), 142–147 (2005).
24. Thewlis, J. Neutron Radiography. *British Journal of Applied Physics*. **7**, 345–350 (1956).
25. Anderson, J. Neutron Radiography in Man. *British Journal of Radiology*. **37**, 957–958 (1964).
26. Brown, M., Parks, P. B. Neutron radiography in biologic media: techniques, observations, and implications. *American Journal of Roentgenology*. **106** (3), 472–485 (1969).
27. Metzke, R. W., Runck, H., Stahl, C. A., Schillinger, B., Calzada, E. Neutron computed tomography of rat lungs. *Physics in Medicine and Biology*. **56** (1), N1–N10 (2011).
28. Crow, L. et al. The CG1 instrument development test station at the high flux isotope reactor. *Nuclear Instruments and Methods in Physics Research, Section A: Accelerators, Spectrometers, Detectors and Associated Equipment*. **634** (1), S71–S74 (2011).
29. Santodonato, L. et al. The CG-1D neutron imaging beamline at the Oak Ridge National Laboratory High Flux Isotope Reactor. *Physics Procedia*. **69**, 104–108 (2015).
30. Grünzweig, C., Frei, G., Lehmann, E., Kühne, G., David, C. Highly absorbing gadolinium test device to characterize the performance of neutron imaging detector systems. *Review of Scientific Instruments*. **78** (5), 1–4 (2007).
31. Schindelin, J. et al. Fiji: An open-source platform for biological-image analysis. *Nature Methods*. **9** (7), 676–682 (2012).
32. Meagher, M. J., Parwani, R. N., Virdi, A. S., Sumner, D. R. Optimizing a micro-computed tomography-based surrogate measurement of bone-implant contact. *Journal of Orthopaedic Research*. **36** (3), 979–986 (2018).

33. Dalesio, L. R. et al. The experimental physics and industrial control system architecture: past, present, and future. *Nuclear Inst. and Methods in Physics Research, A*. **352** (1–2), 179–184 (1994).
34. Bilheux, J., Lin, J. Y. Y., Bilheux, H. Z. Jupyter notebooks for neutron radiography data processing and analysis. *Neutron Radiography-WCNR-11*. **15**, 198–204 (2020).
35. Stalling, D., Westerhoff, M., Hege, H. C. Amira: A highly interactive system for visual data analysis. *Visualization Handbook*. **1**, 749–767 (2005).
36. Tremsin, A. S. et al. Improved efficiency of high resolution thermal and cold neutron imaging. *Nuclear Instruments and Methods in Physics Research, Section A: Accelerators, Spectrometers, Detectors and Associated Equipment*. **628** (1), 415–418 (2011).
37. Tremsin, A. S., Vallerga, J. V., McPhate, J. B., Siegmund, O. H. W. Optimization of high count rate event counting detector with microchannel plates and quad Timepix readout. *Nuclear Instruments and Methods in Physics Research, Section A: Accelerators, Spectrometers, Detectors and Associated Equipment*. **787**, 20–25 (2015).
38. Vlassenbroeck, J. et al. Software tools for quantification of X-ray microtomography at the UGCT. *Nuclear Instruments and Methods in Physics Research, Section A: Accelerators, Spectrometers, Detectors and Associated Equipment*. **580** (1), 442–445 (2007).
39. Gürsoy, D., De Carlo, F., Xiao, X., Jacobsen, C. TomoPy: A framework for the analysis of synchrotron tomographic data. *Journal of Synchrotron Radiation*. **21** (5), 1188–1193 (2014).
40. Pelt, D. M. et al. Integration of TomoPy and the ASTRA toolbox for advanced processing and reconstruction of tomographic synchrotron data. *Journal of Synchrotron Radiation*. **23** (3), 842–849 (2016).
41. Venkatakrishnan, S. V., Cakmak, E., Billheux, H., Bingham, P., Archibald, R. K. Model-based iterative reconstruction for neutron laminography. *Conference Record of 51st Asilomar Conference on Signals, Systems and Computers, ACSSC 2017*. doi: 10.1109/ACSSC.2017.8335686 (2018).
42. Trtik, P. et al. Improving the spatial resolution of neutron imaging at Paul Scherrer Institut - The Neutron Microscope Project. *Physics Procedia*. **69**, 169–176 (2015).
43. Morgano, M. et al. Unlocking high spatial resolution in neutron imaging through an add-on fibre optics taper. *Optics Express*. **26** (2), 9–12 (2018).

Figure1

Click here to access/download;Figure;Figure_1.tiff

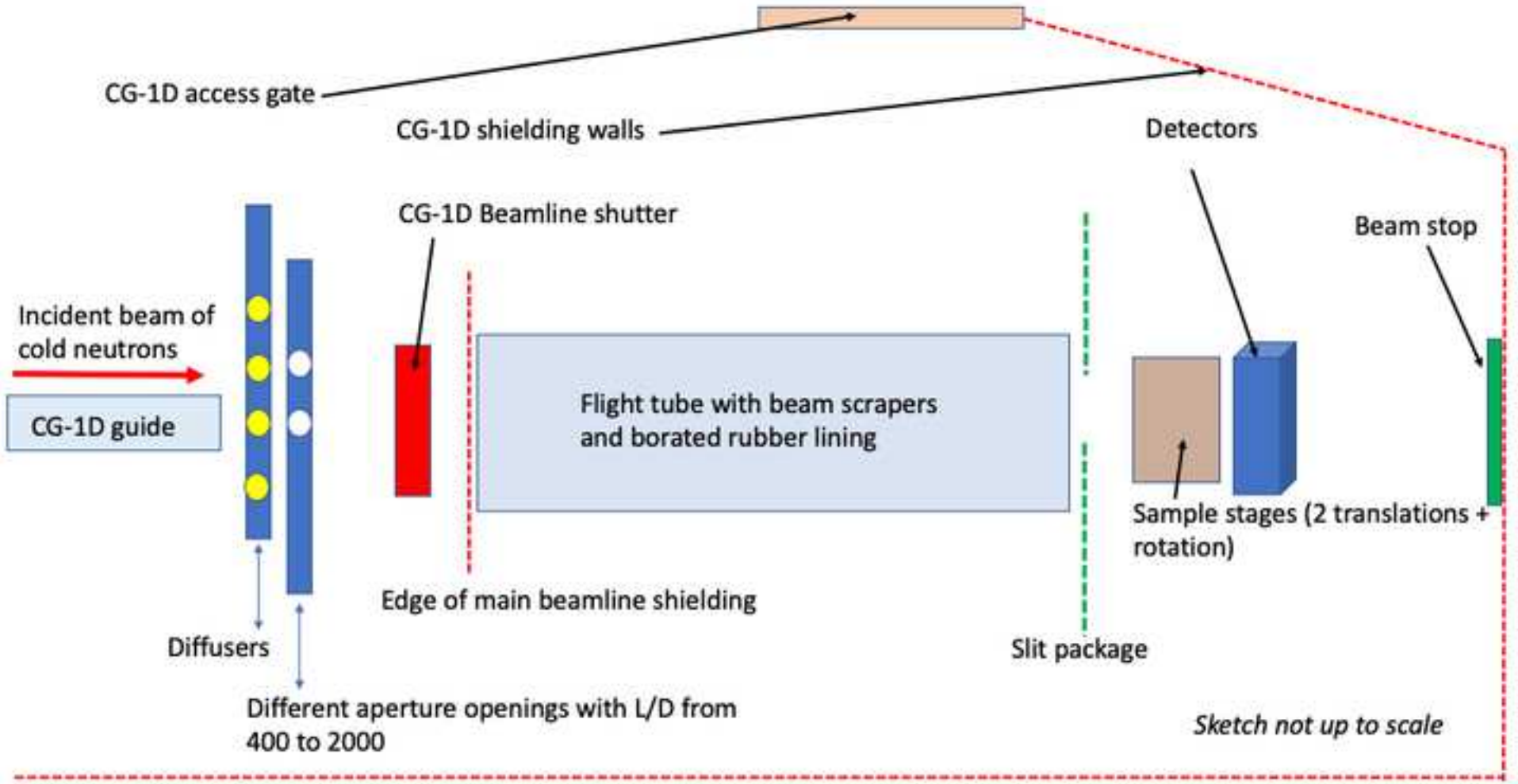

Figure2

Click here to access/download;Figure;Figure_2.tiff

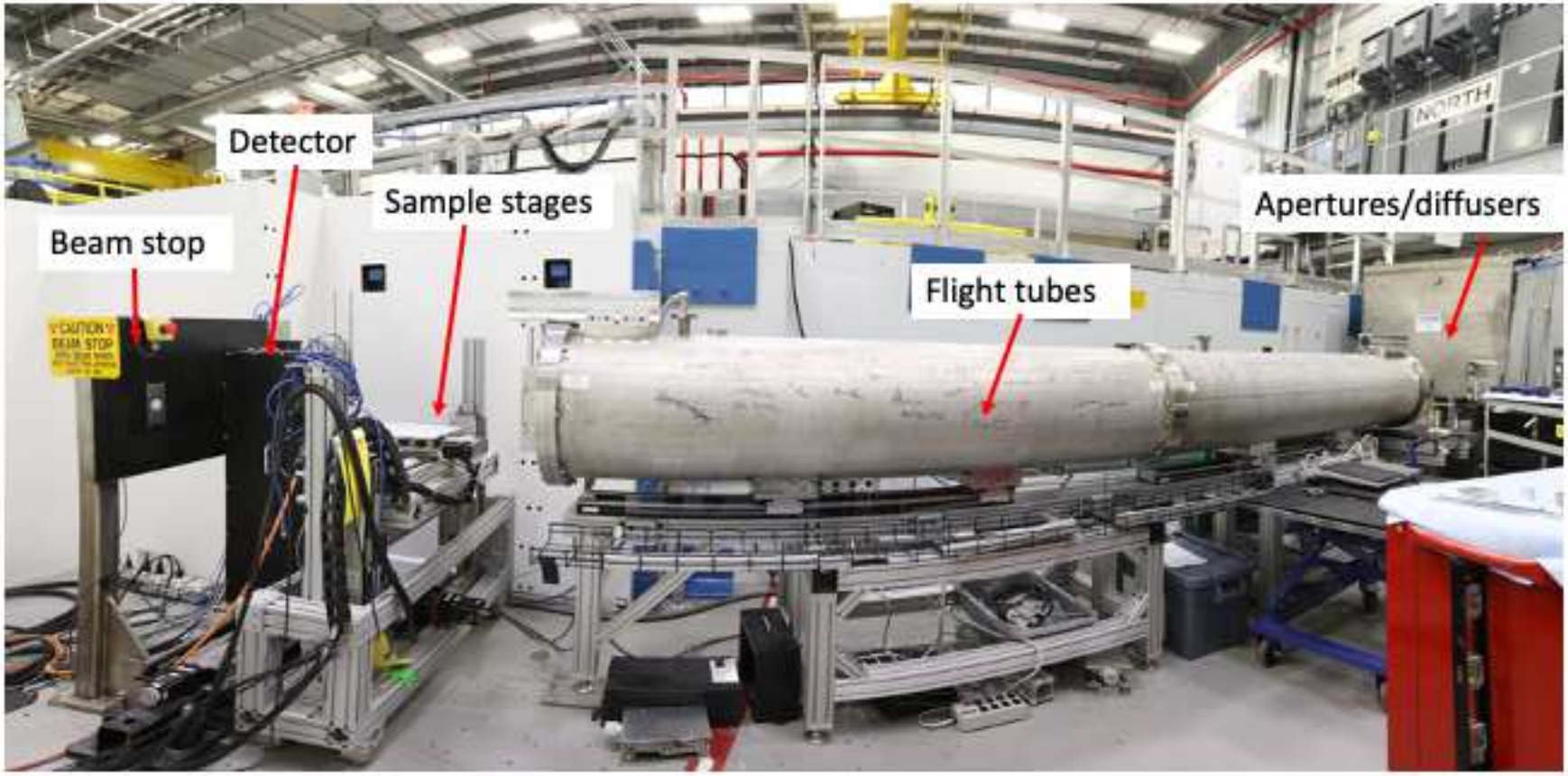

Figure3

Click here to access/download;Figure;Figure_3.tiff

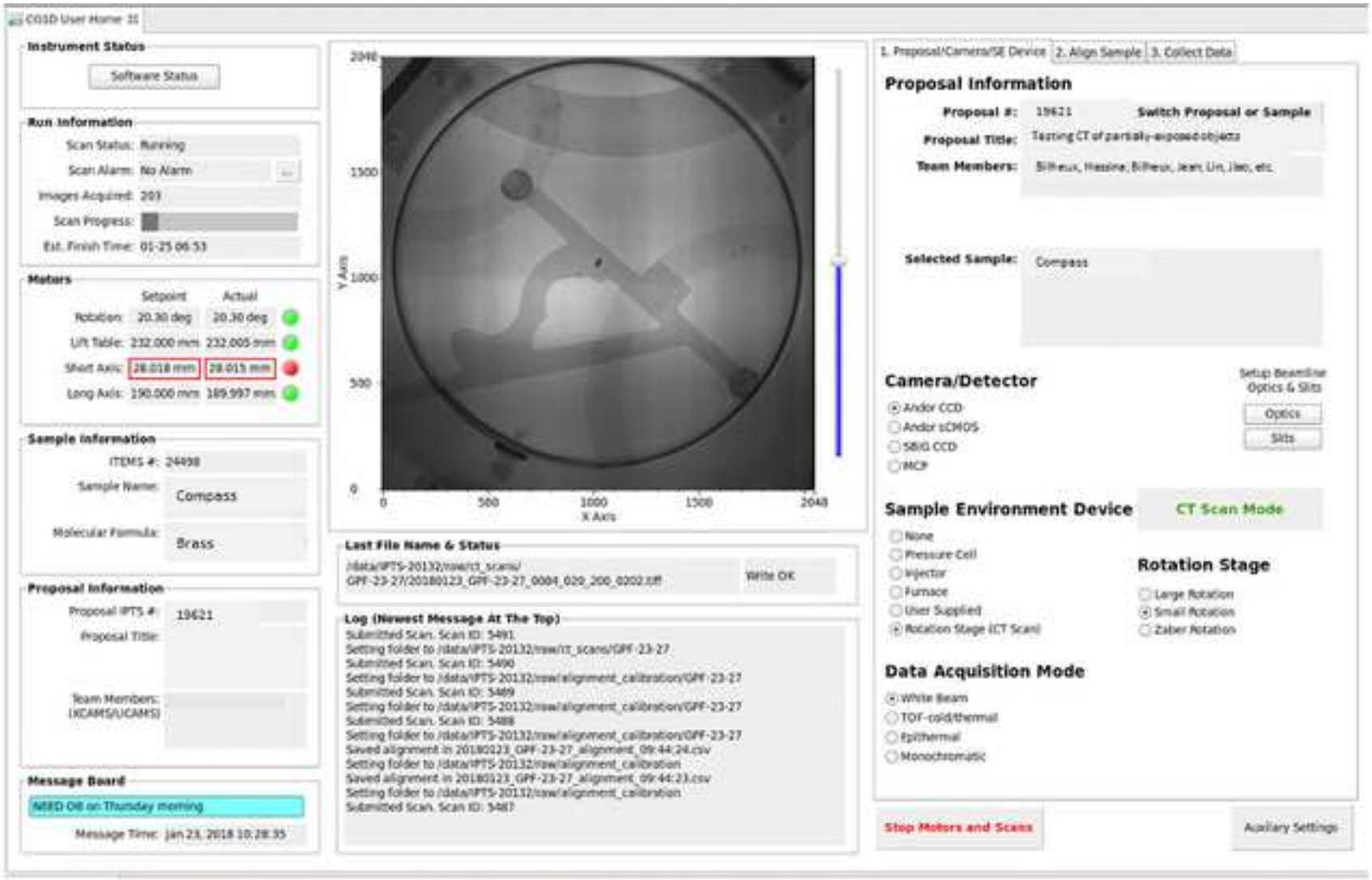

Figure4

Click here to access/download;Figure;Figure_4.tiff

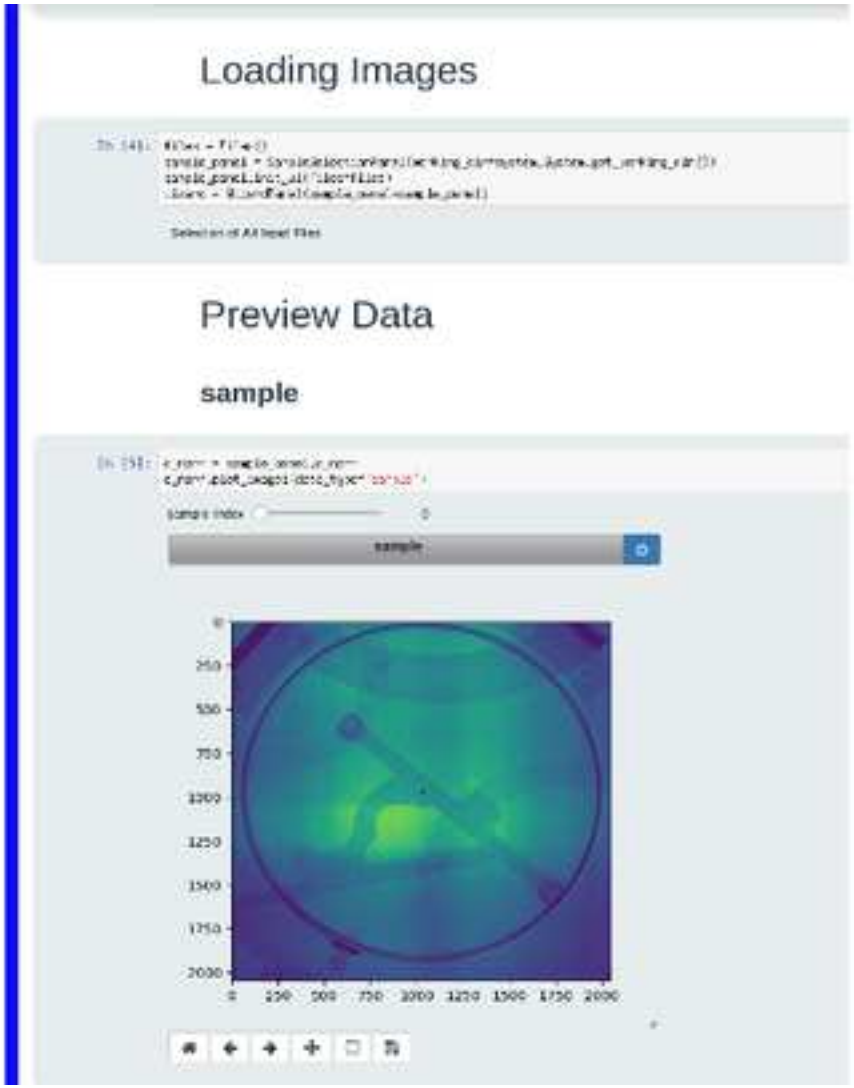

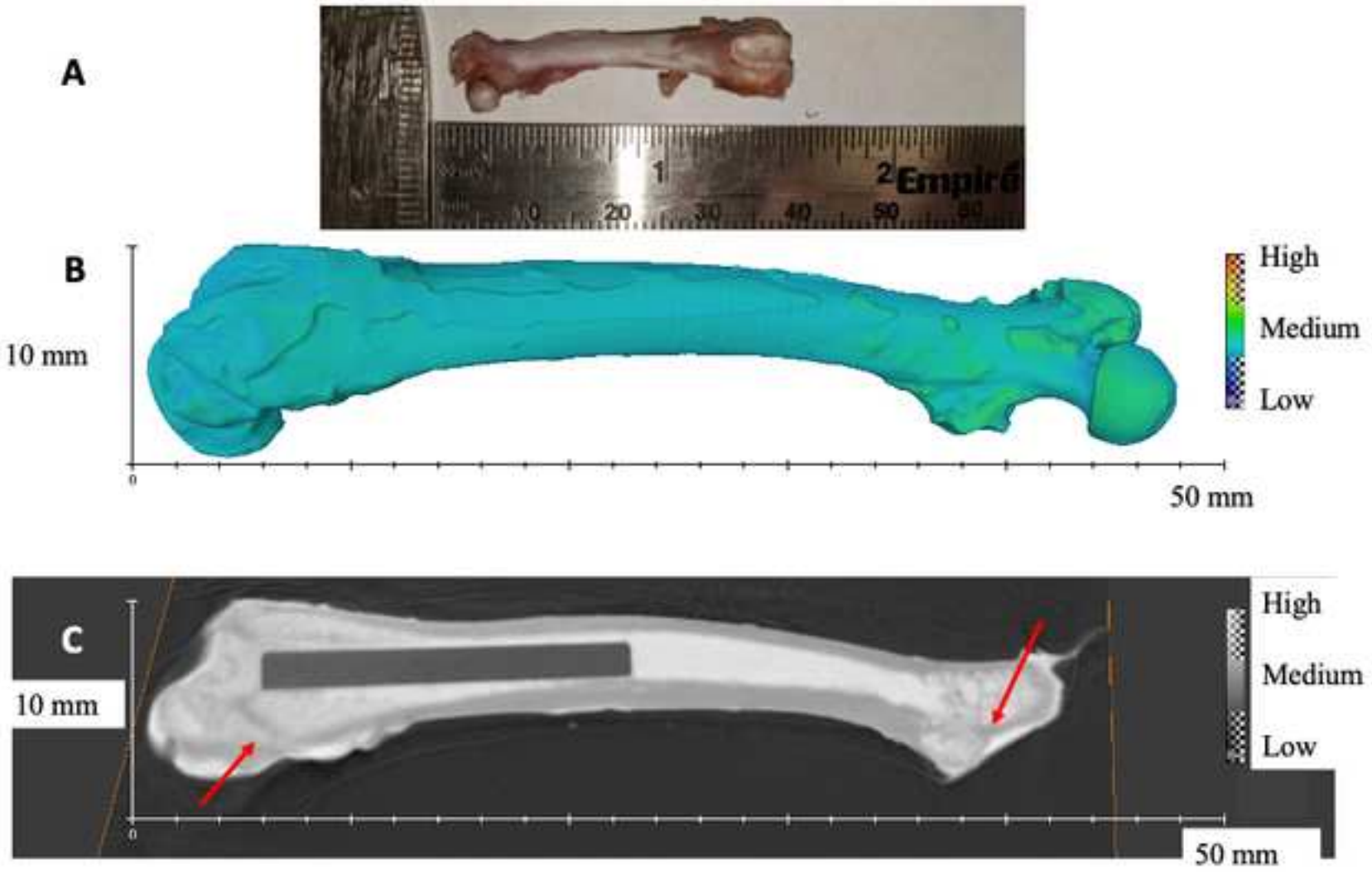

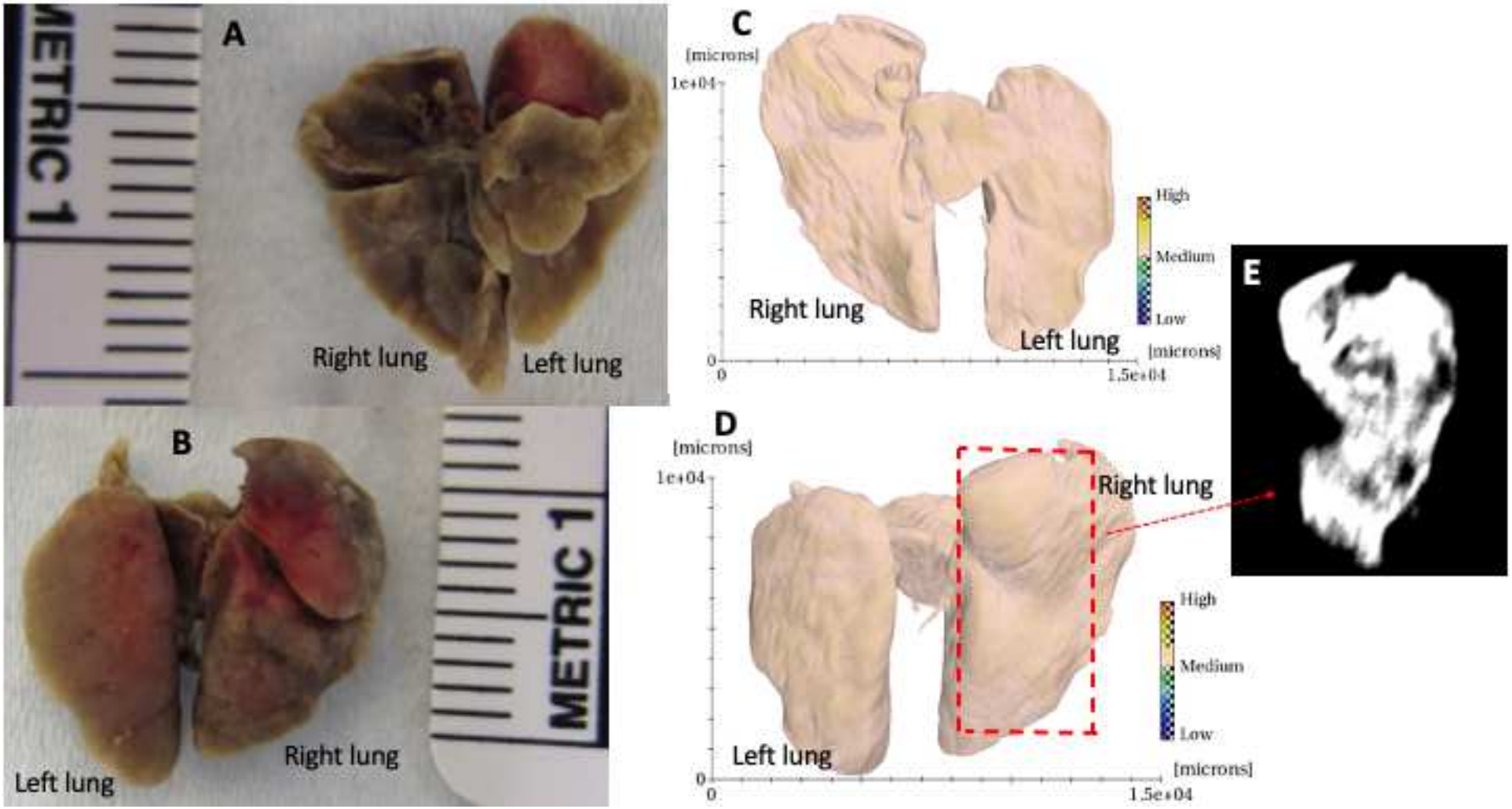

Figure7

Click here to access/download;Figure;Figure_7.tiff

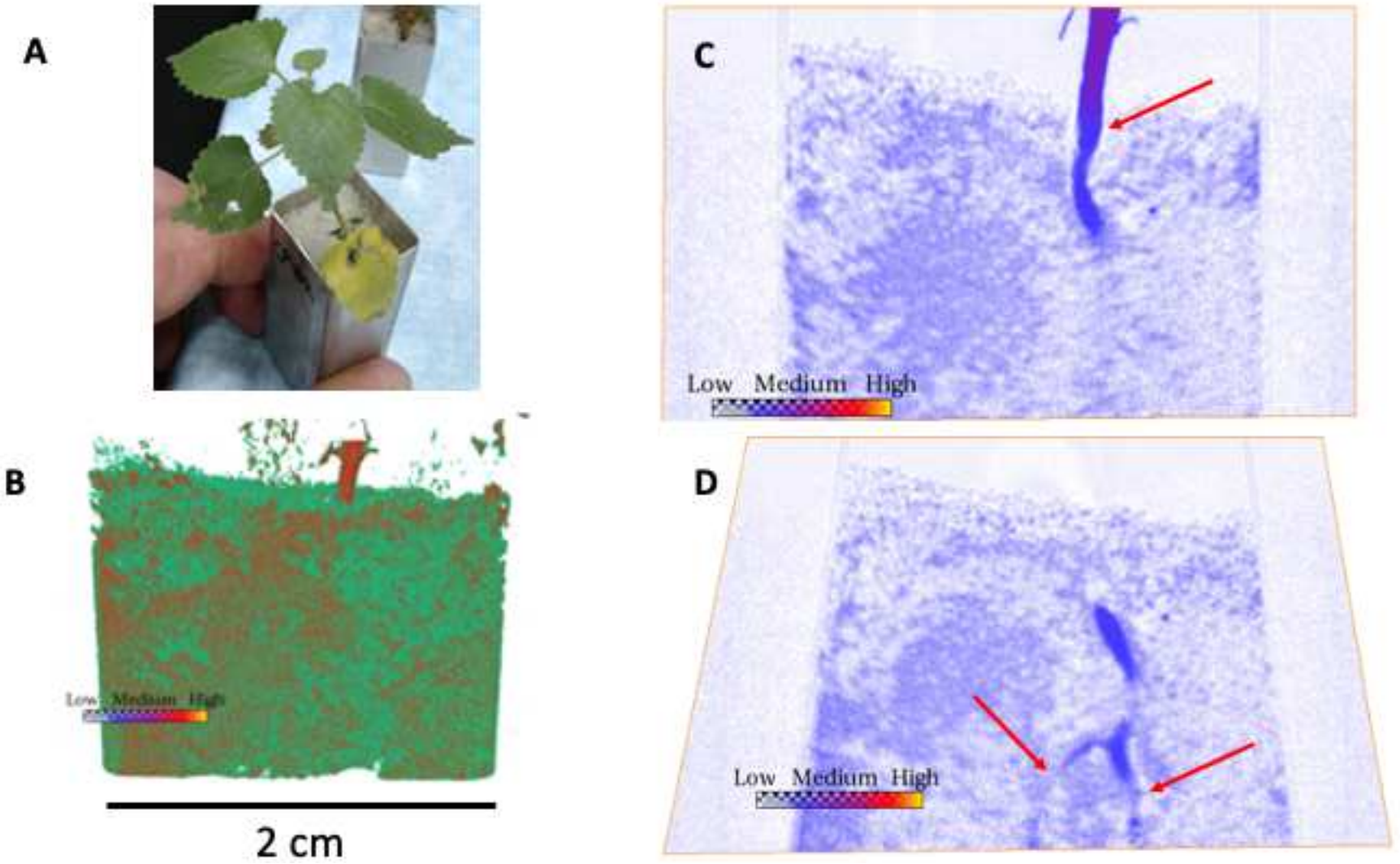

Table of Materials

Name of Material/ Equipment	Company	Catalog Number
Aluminum containers	custom	
Aluminum foil	Fisher	01-213-100
Deionized water or deuterium oxide		
Ethanol	Fisher	04-355-223
Gauze sponges	CardinalHealth	
Growth chamber	Conviron	A1000
Laboratory balance		
Pure silica sand	US Silica Co.	Flint#13
Sprague-Dawley Rats	Harlan	US
Titanium Rod	Goodfellow	TI007905

Comments/Description
Made from aluminum plates or tubing (alternate is quartz), plant and mouse sample Mouse lung sample containment
Water or D_2O can be used to enhance contrast, plant sample Mouse lung sample
Fully submerged in phosphate-buffered saline (PBS) and used to wrap samples, rat femur sample Any growth chamber or greenhouse with controlled conditions would work, plant sample Weighing plant system can be used to measure actual water content in the soils, plant sample Pure SiO_2 provides low neutron attenuation compared to soils, plant sample Rat femur sample Rat femur sample

Dear editor,

Thank you for allowing us to submit the manuscript by December 11, 2020. Please find below our response to the reviewers. We have revised the manuscript according to their suggestions. We kept track of our revisions.

Looking forward to hearing from you.

Best wishes,

Hassina Bilheux on behalf of the co-authors

Please note that novelty is not a requirement for publication and reviewer comments questioning the novelty of the article can be disregarded.

Editorial comments:

Dear editor,

Thank you for your comments and guidance. See our response below.

Changes to be made by the Author(s):
1. Please take this opportunity to thoroughly proofread the manuscript to ensure that there are no spelling or grammar issues.
Done.

2. Please adjust the numbering of the Protocol to follow the JoVE Instructions for Authors. For example, 1 should be followed by 1.1 and then 1.1.1 and 1.1.2 if necessary. Please refrain from using bullets or dashes.
Done.

3. Please move the statement about ethics committee approval from 1.2 to before the numbered protocol steps, indicating that the protocol follows the guidelines of your institution's animal research ethics committee. Did you get the approval for implantation into the rat femurs?
The statement about the ethics committee approval has been moved to *Section 2. Data acquisition.*

Commented [BHZ1]: @Ryan Ross: this needs your attention. I marked in the text where the statement should be made. Thanks.

4. Please ensure that all text in the protocol section is written in the imperative tense as if telling someone how to do the technique (e.g., "Do this," "Ensure that," etc.). The actions should be described in the imperative tense in complete sentences wherever possible. Avoid usage of phrases such as "could be," "should be," and "would be" throughout the Protocol. Any text that

cannot be written in the imperative tense may be added as a “Note.” However, notes should be concise and used sparingly. Please include all safety procedures and use of hoods, etc.
Done.

5. The Protocol should contain only action items that direct the reader to do something. Please move the discussion about the protocol to the Discussion.
Done.

6. Please note that your protocol will be used to generate the script for the video and must contain everything that you would like shown in the video. Please add more details to your protocol steps. Please ensure you answer the “how” question, i.e., how is the step performed? Alternatively, add references to published material specifying how to perform the protocol action. Please add more specific details (e.g., button clicks for software actions, numerical values for settings, etc) to your protocol steps. There should be enough detail in each step to supplement the actions seen in the video so that viewers can easily replicate the protocol.
Done.

7. Please revise the protocol to break it into the main sections (using only the imperative tense for the steps): neutron source and beamline setup, specimen preparation, data acquisition for each specimen, volume reconstruction and data processing. Please include enough details for each procedure so that the steps can be filmed for the entire process for each specimen. After revising, please highlight up to three pages of text for filming.
Done.

8. Step 1 of the instrument setup: what are the pinhole aperture size and opening of the slit system?
The pinhole aperture is what defined the beam geometry and it is mentioned in the manuscript. Since this is the protocol, we don’t explain what each component is again, per your recommendation.

9. Step 2: How are the XY stages installed?
Revised to explain how to do this.

10. Step 3a: How and what lens is selected for sCMOS and how do you focus the camera?
Thank you for your comment. We revised the protocol accordingly.

11. Step 3b: What is involved in using a resolution mask to tune the focus?
Explained.

12. Step 4: How do you secure the sample and use neutron shielding?
The samples are positioned at the beamline in containers, often Al cylinders. Neutron shielding is placed against the detector. We have now clarified this in the manuscript.

13. Step 5: How is pixel size evaluated with the resolution mask?

Pixel size is evaluated by measuring a known feature dimension on the radiograph. Then, by knowing the number of pixels across a dimension, one can determine the size of the pixel. We revised the protocol accordingly.

14. Step 7: How do you align the sample with the neutron beam using the EPICS interface?
Thanks for making this comment. We revised to explain that this is done by taking a series of fast radiographs until the sample is in full view of the detector.

15. 1.1: How much saline-soaked gauze is used to freeze the implants? How is this done?
We use Curity Gauze Sponges, 2 in x 2 in (CardinalHealth, part number 2146), fully submerge them in phosphate buffered saline (PBS) and wrap each sample fully. The manuscript has been revised accordingly.

16. What do you mean by "it was position spending up on the rotation stage…"?
Our apologies, we meant that the sample was positioned sitting up or vertically. We corrected the manuscript, thank you for catching this error.

17. What do you mean by "water was periodically added"—please specify the frequency.
We have expanded the description of plant propagation and watering to indicate that during propagation water is applied daily based on mass loss of the plant system, which allows for precise control of the hydration within the soil.

18. Please rewrite the EPICS data acquisition protocol to specify the various parameters to be entered and selected, which will facilitate filming.
Done.

19. Please remove the embedded figure(s) from the manuscript. All figures should be uploaded separately to your Editorial Manager account. Each figure must be accompanied by a title and a description after the Representative Results of the manuscript text. Please include only Figure Legends after the Representative Results.
Done.

20. Please reorder the figure legends so that fig 1's legend appears first.
Done.

21. Please sort the Materials Table alphabetically by the name of the material.
Done.

Reviewers' comments:
Reviewer #1:

Dear reviewer,
Thank you for your comments. We value your input and have done our best to respond to your review comments and suggestions. Please see below our response below in green.

Manuscript Summary:
The manuscript details how neutron CT on biological samples is performed on the CG-1D beamline at the High Flux Isotope Reactor, Oak Ridge National Laboratory. Measurements can be tailored to different sample types. In particular, dynamics (on the time scale of hours) can be studied, at the cost of signal to noise ratio. Three representative samples are showcased: 1) a rat femur, 2) a mouse lung, and 3) dynamic water uptake in a root system. Overall, the methods are detailed, and the manuscript is well-written.

Minor suggestions:
Line 96 - The microscopic cross section appearing in Eqn. 2 should be called the "total collision cross section" - (diffuse plus absorption cross sections), as opposed to the "total cross section", which could be confused with the "total scattering cross section" (coherent plus incoherent cross sections). For a thorough treatment, see Chapter 4 of Sears, Neutron Optics.
Thank you for this comment. We believe that calling the total neutron cross section can lead to confusion. Thus, we decided to use *neutron attenuation cross section*, as enunciated in the ASTM E1316-17a standard terminology for nondestructive examinations.

Line 118 - many authors have discussed the complementarity of neutron and x-ray CT. I would suggest referencing a review such as Strobl, et al. 2009. Journal of Physics D: Applied Physics, 42(24), 243001. Additionally, the complementarity of neutrons and x-rays is very-well showcased by the simultaneous Neutron and X-ray Tomography (NeXT) system, at the National Institute of Standards and Technology, as described in LaManna et al. 2017. Review of Scientific Instruments 88(11), 113702.
Thank you for the suggestion. These references have been also added. We added Tengattini's NeXT (same facility name as NIST but at ILL) Nuclear Instr. And Methods A 2020 manuscript.

Line 366 - The claim of 100 um resolution is not very-well motivated. Is there a specific structure in Fig 4E that demonstrates this spatial resolution? A scale bar in Fig 4E and/or a more thorough description in the text would solve the problem.
Our resolution is based on Nyquist's theorem, i.e., the spatial resolution is approximately 3 times the pixel. Here, the pixel size is approximately 36 μm. These measurements are done with a SIEMENS star during calibration of the instrument (not during the CT scan). We have added a reference to the resolution mask we use at the beamline (in the protocol section).
A dimension scale is available on the x and y axes (10 mm x 50 mm). Thank you for noticing that the x-scale has been cropped on Figure 5C. It has been corrected. The scale bars are also indicated on the x and y axes. We added a comment in the figure caption for clarification purposes.

Line 493 - The authors should state how long it takes to complete a complementary scan using either a synchrotron or laboratory x-ray source. It is implied that x-ray CT would take much less time, but many readers might not recognize that.
It really depends on the XCT scanner and what resolution is required. We revised the sentence to provide an idea of the time and field-of-view for synchrotron radiation: "This is mostly due to the difference in overall neutron flux available at a reactor compared to a synchrotron source, where X-ray CT scans can take seconds to minutes for a few mm^2 field-of-view."

Reviewer #2:

Dear reviewer,
Thank you for your comments. We value your input and have done our best to respond to your review comments and suggestions. Please see below our response below in green.

Manuscript Summary:
The manuscript describes the workflow for image acquisition and data analysis at the CG-1D neutron imaging beamline at ORNL and demonstrates some imaging applications for biological systems

Major Concerns:
The introduction is very ONRL focused it should be more general even though the purpose of the publication is to describe the workflow at ONRL. It should be extended with some more references to investigation of anatomical structures. E.g., Bone-metal studies have been done by Isaksson, Tudisco, and Le Cann which should be mentioned in the introduction. Lung studies were done at FRM-II before the cited works.
It is also a pity that there are no reports about end applications, the authors mainly show that you can make nice images with neutrons, but not how they can be used in a quantitative analysis.
We thank you for your comments. It is true, indeed, that our manuscript focuses on neutron radiography and computed tomography at ORNL, so we revised our title to reflect this. Our goal was to illustrate how we perform experiment at our facility, rather than a general overview. It now reads "Neutron Radiography and Computed Tomography of Biological Systems at The Oak Ridge National Laboratory's High Flux Isotope Reactor". Thank you for pointing the references out. We have added them to the introduction.

Minor Concerns:
Page 4: Lines 197-201: Don't you do (a) and (b) with the CCD?
The reviewer is correct. We can do this for both detectors (CCD and sCMOS), however in this case, the CCD was already setup, so we did not need to tune it. For completeness and comprehension, we will put both detectors in sections (a) and (b).

Page 5: Line 236: What kind of scintillator did you use and what was the neutron flux? Why do you over scan to 182deg? I hope you don't have a fan angle of 2 degrees when you need 150s exposure time. Over scan is anyway only relevant when you do cone/fan beam reconstruction. Also, didn't the camera saturate with 150s exposures? Did you sum up multiple acquisitions?
We use a cone beam geometry. We've tried both a parallel beam and a cone beam reconstruction using commercial software at the early stages of the facility. The camera did not saturate since we used a 25 μm thick LiF/ZnS scintillator, the only thickness available at the time. Now, we have thicker scintillators, and the camera does saturate in less than 60 s. We have added the scintillator description in the *Neutron source and beamline setup* section.

Page 7 line 322 don't you use something more sophisticated than median filtering to remove spots? What algorithm are you using to remove ring artefacts?
Median filter is adequate since the affected pixels are limited. In the iMARS3D CT reconstruction workflow, two different algorithms can be used for ring artifact removal

1. An algorithm implemented in tomopy that works on the reconstructed images. I did not find a reference for that algorithm
2. The Ketcham algorithm we implemented that works on the sinograms. The original paper of Ketcham is here https://doi.org/10.1117/12.680939

We can also use AMIRA for ring filtering after the reconstruction has been performed and slices have been generated (https://www.thermofisher.com/us/en/home/industrial/electron-microscopy/electron-microscopy-instruments-workflow-solutions/3d-visualization-analysis-software/amira-life-sciences-biomedical.html).

Reviewer #3:

Dear reviewer,
Thank you for your comments. We value your input and have done our best to respond to your review comments and suggestions. Please see below our response below in green.

Manuscript Summary:
This manuscript describes the protocol to perform neutron radiography and computed tomography of three biological samples at the High Flux Isotope Reactor (HFIR) CG-1D beamline.

Major Concerns:
* The title is too general, the work presented here is from a specific facility HFIR from Oak Ridge, so I'd recommend changing the title to clearly emphasize where this work was done, e.g. Neutron Radiography and Computed Tomography of Biological Systems at HFIR, Oak Ridge. If the authors want to keep their title, then they have to add references to what has been done on this topic (biological systems) at other neutron imaging facilities (from UK, Switzerland, Germany) on biological systems.
This is a very good point. We did change the title to: “” and we added references from colleagues in Europe in the introduction section (Schillinger in Germany, Burca et al. in the UK, and Kaestner in Switzerland). Thank you for the comment.

* Line 118: The authors say 'This manuscript aims to demonstrate that neutron imaging (nR and nCT) is a complementary technique to X-ray imaging' but unfortunately nothing from X-ray imaging measurements/ protocol is presented here to prove the claim. Entire manuscript is based only on neutron imaging results.
Excellent point. This is a remnant to our original manuscript. Once we had a better understanding of the manuscript focus (in order to publish videos), we changed our initial focus. We have rephrased the sentence as follows:

" This manuscript aims to demonstrate the procedure of using neutron imaging (nR and nCT) at HFIR CG-1D beamline." We have moved the comment on the complementarity between neutron and X-ray imaging in the introduction.

Minor Concerns:
1. Line 96: σ_i doesn't appear in equation (2).
Thank you for pointing this out. It should be σ. We have corrected our mistake.

2. Line 202: What kind of material was used for container? What kind of neutron shielding was used for detector and equipment?
Good points. We usually use Al as a container as it mostly does not disrupt the neutron beam. The shielding for the detector is two-fold: boron rubber and Pb bricks, in this order from the beam/sample to the detector. Boron carbide absorbs neutrons but produces gammas. Pb bricks are needed because most samples or sample holders produce gammas. They also scatter neutrons thus the need to absorb them and stop the subsequent gammas too. We have revised the manuscript accordingly.

3. Line 190: 'A photograph of the CG-1D beamline is given in Figure 2' - not true. Please double check the Figure's number
Thank you. Figure 2 now shows a photograph of the facility or CG-1D beamline.

4. Section 1.3.: It is unclear how many samples were measured. Two plants (mulberry weed and mint)? Why mulberry plant was grown in chamber for 1 week? The plant had already 6.3 cm height when it was excavated; How was mint plant prepared before being transplanted in Al container?
Thank you for your comment. The mint plant is not shown in this article, it was a typo that should have been removed before submitting the manuscript. We transplant our plant before the experiment to acclimate them to their new environment (sand) so that water uptake is not measured when the plant is stressed due to the transplant.
We revised the manuscript to indicate the plant preparation, including water cycles and its transplant to the sand soil.

5. Line 242: Is any type of quartz suitable?
Pure polycrystalline quartz is fine. We try to avoid quartz because it is commonly used as glass for chemistry applications and contains a small amount of boron which absorbs neutrons. Ideally, we would measure the container alone to make sure it is not too attenuating. The advantage is the ability to see through which is of interest to plant physiologists.

6. Line 247: How was the water periodically added to maintain the plant during the experiment?
We used a needle that we inserted at the bottom of the Al chamber through a punctured hole. We added water once a day to maintain the plant's health. We revised the manuscript accordingly.

7. Line 516: Why each sample was reconstructed with a different type of reconstruction software?
We used three software packages, one commercial (Octopus) and another based on the open-source code TomoPY. Octopus has been discontinued and the company that created it does not

offer any technical support, so we transitioned to iMARS3D (based on TomoPY). For fast CT (less than 2 hr), we cannot use Octopus nor IMARS3D because they are based on the filtered-back projection method, which requires high signal-to-noise data. Thus, we decided to utilize an iterative method which was more successful than our attempt to use the previously mentioned tools.

8. Line 338: Why is it mentioned only iMARS3D in the protocol steps and not also Octopus or pyMBIR? There is nothing mentioned about the filters (pre- or post-processing filters) in the protocol steps.
Thank you for your comment. We do mention that ring artifacts, median filtering and smoothing are available with our software. We will explicitly demonstrate them during the video. We have added these steps in our protocol for image processing.

9. Line 438: It's Figure 5 instead of Figure 3
Thank you. The figure numbering has been corrected.

10. Line 456: It's Figure 6 instead of Figure 4
Thank you. The figure numbering has been corrected.

11. Line 479: It's Figure 7 instead of Figure 5
Thank you. The figure numbering has been corrected.

Reviewer #4:

Dear reviewer,
Thank you for your comments. We value your input and have done our best to respond to your review comments and suggestions. Please see below our response below in green.

Manuscript Summary:
The manuscript is to demonstrate the neutron radiography and tomography as suitable imaging technique for biological samples. As samples a plant root system, a rat femur implant and a mouse lung. The aim is to demonstrate the applicability of neutron imaging as complementary technique to x-ray imaging. The paper focuses on the advantages of neutron bioimaging as neutrons interact strongly with hydrogen and hydrogen is an abundant material in biological systems.

Major Concerns:
My major concern is the lacking novelty. Neutron imaging to biological systems is applied since longer time. However, when the paper aims to present the methodology without claiming novelty that is okay. Another major concern is that the authors claim to demonstrate neutron imaging as complementary method to x-ray imaging. However, no results on x-ray imaging are shown and the complementary information that are gained are not discussed. Another concern is that the examples that are chosen are not convincing. At first neutron imaging is not non-invasive as gamma radiation could also influence living plants. Also, the plant had to be potted in sand. Furthermore, biological tissues cannot be investigated in vivo but the animals have to be sacrificed for imaging. I don't see the large advantage of neutron imaging in that cases.

Thank you for your comments. We have removed the claim that we are comparing neutrons with X-rays and solely focus the manuscript on neutron imaging. The plants are not damaged by neutron imaging or low energy gammas produced when neutrons are in contact with the Al container. As a matter of fact, plants have survived weeks and months after neutron exposure. The advantage of neutron imaging in animal tissue is the capability to look at thick layers of tissue rather than histology where slices are ~ 7 μm. In the case of neutron CT, samples can be a couple of mm thick, thus being equivalent to measuring hundreds of histology slices. In that sense, nCT is not as invasive and destructive.
In the introduction, we have added references from other teams who have measured similar samples as we did.

Minor Concerns:
Please refer to the complementarity between x-ray und neutron imaging.
Thank you for your recommendation. We have added references that directly compare neutrons and X-ray imaging.

line 233: what was the spatial resolution
The spatial resolution of all our measurements is on the order of 75 μm (see lines 164-167).

Fig. 4 Please provide scale bars with units
Thank you for your recommendation. The scale bars are indicated on the x and y axes. We added a comment in the figure caption for clarification purposes.

Fig. 5 Please use consistent terminology for the presented methods
Thank you. We have changed the terminology of both Figures 6 and 7 to match.

line 308: Is it possible to visualize the mouse lung in-vivo?
Since we used cold neutrons, they are not energetic enough to pass through tissues that are thicker than 2-3 mm. There has been an attempt in the 1960's to visualize human lungs on a live person. See reference: J. Anderson, Neutron Radiography of Man, British Journal of Radiology, Vol. 37, 1964.

line 442: complementarity is not shown
Understood. Removed this part of the discussion.

line 137ff: What is the beam intensity? Please provide
Thank you for your comment. The flux on sample is on the order of 10^7 n/cm^2/s. We have added this value in the *Neutron source and beamline setup* section.

line 240ff: The data acquisition system is very special to the oak ridge laboratory and not of such high use for other neutron sources
Good point. Our manuscript is indeed specific to Oak Ridge, on purpose, as we are trying to illustrate the steps of doing an experiment at our facility. Hence, we have changed the title to reflect this. It now reads: *Neutron Radiography and Computed Tomography of Biological Systems at The Oak Ridge National Laboratory's High Flux Isotope Reactor*

line 452: the chosen examples are not appropriate

Thank you for your comment. The chosen examples were selected because they represent 90% of our scientific community in the biological field. In this sense, these examples are representative of the community that utilizes our facility.